Vortex-vacancy interactions in two-dimensional easy-plane magnets

G. M. Wysin*
Department of Physics, Kansas State University, Manhattan, Kansas 66506–2601
(Dated: July 17, 2003)

For a model with isotropic nearest neighbor exchange combined with easy-plane exchange or single-ion anisotropies, the static effects of a magnetic vacancy site on a nearby magnetic vortex are analyzed on square, hexagonal and triangular lattices. Numerical energy minimization and linear stability analysis using the vortex instability mode are employed. When the vortex is centered on a vacancy, the critical anisotropies where the stable vortex structure switches from out-of-plane to planar form are determined, and the vortex energies and magnetizations are found as functions of anisotropy. Consistent with square lattice calculations by Zaspel et al, the strength of anisotropy needed to stabilize a vortex in the planar form is reduced when the vortex is centered on a vacancy, for all three lattices studied. The vortex-on-vacancy energy is found to be smaller than the typical energy of a vortex centered between lattice sites in a system without vacancies. For a vortex separated from a vacancy, the energy found as a function of separation demonstrates an *attractive* potential between the two.

PACS numbers: 75.10.Hk, 75.30.Ds, 75.40.Gb, 75.40.Mg

I. INTRODUCTION

Magnetic vortices in two-dimensional (2D) systems with easy-plane coupling have attracted a number of investigations related to the structure and stability of the in-plane and out-of-plane vortex types.[1–7] The presence of these two vortex types[1] was found in numerical simulations to exhibit an instability at a critical anisotropy,[2,3] at which one type can transform to the other due to favorable energetics. The instability has been explained in terms of the energy balance and softening of a dynamic mode on a vortex[4,5] using discrete lattice models, with precisely located critical points found by analyzing progressively larger and larger vortex core regions.[6,7]

A magnetic material is likely to have some distribution of magnetically inert or nonmagnetic impurities at some of the lattice sites. Effectively these are magnetic vacancies with respect to the magnetic degrees of freedom. Each vacancy site is expected to play a role in the structure and dynamics of all the magnetic excitations present. Zaspel et al[8] considered a model for such a nonmagnetic impurity in a square lattice 2D ferromagnet (FM). Applying the same discrete core methods as was done for uniform systems, they studied the structure and stability of a vortex centered on a vacancy site on a square lattice. They found that the easy-plane anisotropy strength necessary to keep the vortex in the in-plane form was drastically reduced by the vacancy. The effect is significant: the critical anisotropy strength δ_c (as a fraction of the exchange energy, see definition and Hamiltonian below) was found to change from about 0.2966 for a free vortex to a new value 0.0429 when pinned on a vacancy. It means that in real materials even the presence of a low density of vacancies could dramatically influence the static and dynamic magnetic properties. Further studies have indicated significant dynamic features attributed to vortices pinned on impurities in isotropic antiferromagnets (AFM).[9–11]

On the other hand, Mól et al[12] made a *continuum* calculation for a vortex near a nonmagnetic impurity under the assumption that the impurity produces a certain global deformation of the vortex spin structure. The calculation indicated an effective repulsive potential between a planar vortex and the nonmagnetic impurity. This would suggest that a spin vacancy could not attract or pin a nearby vortex. Then the discrete core model for the calculation of critical anisotropy would be of questionable value. Monte Carlo simulations of a planar rotator model[13] indicated a lowering of the Berezinskii-Kosterlitz-Thouless transition temperature[14] due to the presence of magnetic vacancies. Using a continuum model, Leonel et al[13] concluded that a nonmagnetic impurity will repel either an individual vortex or even a vortex-antivortex pair, and that this effect can even force the BKT transition temperature to zero at a critical density of vacancies. On the other hand, studies of a 2D isotropic Heisenberg antiferromagnet by Mól et al[15] and Pereira[16] determined oscillatory dynamic modes of solitons pinned to vacancies, which requires an attractive restoring potential. These are contradictory results, therefore, further investigation of the vacancy–vortex interaction potential is needed.

Although these are related but distinct models (three-component easy-plane, one-component planar, and AFM vs. FM), it would be satisfying to understand better the vortex–vacancy interaction problem in general, partly to resolve this discrepancy, and to gain a better understanding of the overall energetics and the influence of different lattices. The studies here will involve only lattice models; they may give some insight when compared to the above mentioned continuum predictions. Ultimately a lattice model for a vacancy is the original source of any continuum theoretical description; the continuum theory cannot completely describe subtle differences ocurring on the different lattices at short length scales. In this regard, the vortex–vacancy interaction is studied here on

2D square, hexagonal and triangular lattices.

For simplicity, we consider the effect of a single vacancy on a single magnetic vortex. The static structure and properties of the vortex are found when the vortex is centered on the vacancy. Additionally, an effective vortex-vacancy interaction potential is estimated as a function of their separation. It is found that the vortex–vacancy interaction potential is always attractive, and that at well-chosen anisotropy, the dynamic process of pinning of a vortex onto a vacancy could lead to strong out-of-plane spin fluctuations at very low energy cost.

II. EASY-PLANE MODEL

The model to be investigated has classical spins defined at lattice sites $\mathbf{n}$ interacting with nearest neighbors at displacements $\mathbf{a}$ according to the Hamiltonian,

$$H = J\sum_{\mathbf{n}}\Big\{-\frac{1}{2}\sum_{\mathbf{a}}\Big[S^x_{\mathbf{n}}S^x_{\mathbf{n+a}}+S^y_{\mathbf{n}}S^y_{\mathbf{n+a}}+\lambda S^z_{\mathbf{n}}S^z_{\mathbf{n+a}}\Big]+d(S^z_{\mathbf{n}})^2\Big\}. \tag{1}$$

Parameter λ determines the exchange anisotropy strength $\delta \equiv 1-\lambda$ and d is the single ion anisotropy strength. Positive values of δ and d correspond to the easy-plane anisotropy that is of interest here. The z-axis is the hard axis; xy is the easy plane. A ferromagnetic interaction is assumed. For static vortex properties, there are essentially no differences in energy or critical anisotropies for the antiferromagnetic model on square and hexagonal (bipartite) lattices. The vortex structure in terms of staggered magnetization for AFM vortices is the same as that for FM vortices with the same anisotropy parameters. Obviously these comments do not apply to the AFM model on the triangular lattice, due to each site having six nearest neighbors, requiring three sublattices, which results in frustration. With this exception, study of the FM model is sufficient for determining the static vortex properties. Dynamic properties, however, *will* be different for AFM vs. FM models.

A. Vortices in a Uniform System

It is convenient to write the spins of length S in terms of in-plane angles $\phi_{\mathbf{n}} \equiv \tan^{-1}(S^y_{\mathbf{n}}/S^x_{\mathbf{n}})$ and scaled out-of-plane component $m_{\mathbf{n}} \equiv S^z_{\mathbf{n}}/S$,

$$\vec{S}_{\mathbf{n}} = S(\sqrt{1-m^2_{\mathbf{n}}}\cos\phi_{\mathbf{n}}, \sqrt{1-m^2_{\mathbf{n}}}\sin\phi_{\mathbf{n}}, m_{\mathbf{n}}). \tag{2}$$

In this notation a static vortex at position $\vec{r}_v = (x_v, y_v)$ in *continuum* theory has in-plane angle in the configuration

$$\phi(\vec{r}) = \Phi^v(\vec{r}) = \tan^{-1}\left(\frac{y-y_v}{x-x_v}\right)+\phi_0, \tag{3}$$

where ϕ_0 is an arbitrary constant, set to zero here without loss of generality. On a lattice, the in-plane vortex angles $\Phi^v_{\mathbf{n}}$ lose the perfect circular symmetry of this formula, and obtain modifications largest near the vortex core. They satisfy a discrete lattice nonlinear Laplace equation,

$$\sum_{\mathbf{a}}\sin(\Phi^v_{\mathbf{n}}-\Phi^v_{\mathbf{n+a}}) = 0. \tag{4}$$

(The same equation will give the vortex structure also when a vacancy exists.) The out-of-plane component m satisfies an appropriate energy minimization equation resulting from H.

It is well known that two vortex types (out-of-plane, at weak anisotropy, and in-plane, at stronger anisotropy) can be present in this model. The out-of-plane vortex has a nonzero profile for $m_{\mathbf{n}}$ whose magnitude typically peaks somewhere near the vortex core, and diminishes over a length scale determined by the inverse anisotropy strength. The in-plane or planar vortex has $m_{\mathbf{n}} = 0$ everywhere. The in-plane vortices require a minimum anisotropy strength (denoted by critical parameters λ_c or d_c for the different forms of anisotropy) in order to be stabilized. Conversely, the out-of-plane vortices are stable only if the anisotropy is weaker than the critical value. For a vortex centered in a plaquette (between lattice sites), the critical anisotropy strength for in-plane vortex stabilization increases with the coordination number (z) of the lattice.[6] For hexagonal ($z = 3$), square ($z = 4$) and triangular ($z = 6$) lattices, the respective critical values are $\delta_c \approx 0.1670, 0.2966, 0.3871$ and $d_c \approx 0.2212, 0.4690, 0.8391$. Additionally, there is a weak attractive potential pulling the vortex center to a position of high symmetry at the center of a plaquette. In the present study, we investigate how the presence of a vacancy could modify the critical anisotropies for the different lattices, and how a vacancy otherwise affects the vortex structure and energetics.

III. VORTEX ON A VACANCY

A system is considered with a single magnetic vacancy at its center, which is taken as the origin of coordinates, $(0, 0)$. The center of the vortex is coincident with the vacant site. For the purpose of analysis and numerical calculations, a finite circular system of radius R is considered, on either hexagonal (i.e., honeycomb), square or triangular lattices. This means lattice sites are set up surrounding the origin, according to the chosen lattice, and only those within radius R are kept. The system is abruptly cut off at radius $r = R$; effectively it is a system with a free boundary condition at this radius. The missing magnetic site corresponds to a number of missing exchange bonds equal to the coordination number of the lattice, $z = 3, 4, 6$ for hexagonal, square or triangular lattices. Thus, the order of magnitude of the energy change due to a vacancy should be proportional to zJS^2.

A. Critical Anisotropy Calculations

The critical anisotropies are determined by locating the values where it becomes energetically favorable for the in-plane vortex to develop nonzero out-of-plane components. The method used in Refs. 6, considering a set of core spins that is most important in the energetics, is applied here. Each spin is assumed to have small amplitude dynamic deviations from the in-plane vortex structure:

$$\phi_{\mathbf{n}} = \Phi^v_{\mathbf{n}} + \varphi_{\mathbf{n}}, \quad S^z_{\mathbf{n}} = S m_{\mathbf{n}}. \tag{5}$$

The linearized equations of motion for the fluctuations φ and m produce a zero-frequency normal mode when the anisotropy strength is at a critical value. The mode obtains an imaginary frequency when the anisotropy strength is weaker than the critical value, signifying the growth of nonzero out-of-plane spin components, and the transition to an out-of-plane vortex structure.

1. Ring Coordinates on Different Lattices

For the vortex instability mode, all sites related by symmetry operations appropriate to the lattice have the same in-plane and out-of-plane spin fluctuations. This general idea was used in previous calculations[4,7,8] and the symmetry related sites have been refered to as rings.[6] Because the vortex is assumed to be centered on the vacancy, rather than centered in a plaquette, the new ring definitions for the vacancy problem are given here.

On a **square lattice**, the rings can be defined using principal sites in the first octant of the xy plane (Fig. 1). Around the vacant origin, using lattice constant a, a site at $(x, y) = a(i, j)$ and all its symmetry related sites at $a(\pm i, \pm j)$ and $a(\pm j, \pm i)$ compose a ring. A ring α is defined by a pair of positive integers, $\alpha = (i, j)$. The allowed rings have $i = 1, 2, 3...$ and $j = 0, 1, 2...$ with $j \leq i$; the restriction $i \neq 0$ produces the vacancy. The number of members in a ring will be denoted as μ_α. The rings with $j = 0$ or $j = i$ lie along lines of high symmetry and have only $\mu_\alpha = 4$. All other rings have $\mu_\alpha = 8$. Unlike the uniform system problem, there are no exchange interactions within an individual ring (no intra-ring exchange energy, $E_{\mathrm{ee},\alpha} = 0$). For neighboring rings $\alpha = (i, j)$ and $\alpha' = (i', j')$, the number of exchange bonds between them is denoted by $c_{\alpha,\alpha'}$. One has $c_{\alpha\alpha'} = 4 = z$ when $j = j' = 0$ (both rings' principal sites on the x-axis, a line of high symmetry), and $c_{\alpha\alpha'} = 8 = 2z$ otherwise. Before relaxation to a minimum energy in-plane vortex state, the in-plane vortex angle for principal ring site with (i, j) is simply $\Phi^v_\alpha = \tan^{-1}(j/i)$.

On a **hexagonal lattice**, a set of principal sites within the first sextant of the xy plane define the rings (Fig. 2). With the vacancy at the origin, and using integers $i = 1, 2, 3...$ and $j = 0, 1, 2...$ with $j \leq i$, the sites on a ring lie at principal sites $(x, y) = a(\frac{1}{2}i, \frac{\sqrt{3}}{2}j)$, and other sites related by 120° rotations and reflections across the line $i = j$. The restriction that $(i + j)$ is even produces a triangular lattice and the additional restriction $i - 3j - 2 \neq 6n$, n =integer, removes the hexagon center sites. One can note that the principal ring sites might also be constructed as the positions $\vec{r} = l\hat{a} + j\hat{b}$, where $l = \frac{1}{2}(i - j)$, using basis vectors for hex/tri lattices, $\hat{a} \equiv a(1, 0)$ and $\hat{b} \equiv a(\frac{1}{2}, \frac{\sqrt{3}}{2})$. The rings along major lines of symmetry where $j = 0$ or $j = i$ have number of members $\mu_\alpha = 3$; all other rings have $\mu_\alpha = 6$. There is no intra-ring exchange energy, $E_{\mathrm{ee},\alpha} = 0$. Neighboring rings $\alpha = (i, j)$ and $\alpha' = (i', j')$ along major lines of symmetry $j = j' = 0$ (both along $\hat{a}$ axis) or with $(i - j) = (i' - j')$ (both along $\hat{b}$ axis) have number of exchange bonds $c_{\alpha\alpha'} = 3 = z$. Other neighboring rings have $c_{\alpha\alpha'} = 6 = 2z$. Before relaxation, the in-plane vortex angle for principal ring site (i, j) is $\Phi^v_\alpha = \tan^{-1}(\sqrt{3}j/i)$.

For the **triangular lattice** system, a set of principal sites in the first 30° above the x-axis is sufficient to define the rings (Fig. 3). One needs ring sites as on the hexagonal lattice, with $(x, y) = a(\frac{1}{2}i, \frac{\sqrt{3}}{2}j)$, where $i = 1, 2, 3...$ and $j = 0, 1, 2...$ with the restriction that $(i + j)$ is even. To constrain to the principal sites in the first 30° slice requires $j \leq \frac{1}{3}i$. The rings with principal site along high symmetry lines at 0° ($j = 0$) and 30° ($j = \frac{1}{3}i$) to the $+x$-axis have number of members $\mu_\alpha = 6$; all others have $\mu_\alpha = 12$. The rings such as $(i, j) = (2, 0), (5, 1), (8, 2)$, etc., whose principal sites lie just below the 30° line, satisfying $j = \frac{1}{3}(i - 2)$, have six intra-ring exchange bonds across the 30° line. The intra-ring exchange energy in one of these rings with principal site in-plane vortex angle Φ^v_α and out-of-plane fluctuation m_α is

$$E_{\mathrm{ee},\alpha} \equiv -6JS^2 \left\{ (1 - m^2_\alpha) \cos[2(30° - \Phi_\alpha)] + \lambda m^2_\alpha \right\}. \tag{6}$$

Just as for the hexagonal lattice, neighboring rings $\alpha = (i, j)$ and $\alpha' = (i', j')$ along major lines of symmetry $j = j' = 0$ or with $(i - j) = (i' - j')$ have $c_{\alpha\alpha'} = 6 = z$, and other neighboring rings have $c_{\alpha\alpha'} = 12 = 2z$. The unrelaxed in-plane vortex angle for principal ring site (i, j) is $\Phi^v_\alpha = \tan^{-1}(\sqrt{3}j/i)$.

2. Relaxed Static In-Plane Vortices

It was mentioned in the Introduction that the static in-plane angles satisfy the discrete nonlinear Laplace equation (4), even with a vacancy in the system. This is seen even from minimizing the total energy in the ring coordinates, under the stipulation that all out-of-plane fluctuations $m_\alpha = 0$; see the Hamiltonian in the next section. Therefore, before proceeding to get critical anisotropies, the in-plane vortex structure, as defined using the ring variables, was relaxed to a local minimum energy configuration, consistent with equation (4). This was achieved by an iteration procedure in which each ring angle Φ^v_α was adjusted to point along the effective field of its neighboring rings, scanning through all the active rings, until

the magnetization and energy changes fell below a desired precision. Typically, such a relaxation procedure only makes very minor changes (of the order of 1% or less) in the spin components at sites close to the vortex core. Farther from the core, the relaxed spin angles are well-described by the continuum formula, Eq. (3).

3. Zero-Frequency Dynamic Mode

Denoting neighboring rings as (α, α'), the total system Hamiltonian is written $H = H_{\rm int} + H_{\rm self}$, where the *interaction* and *self* energies that follow from Eq. 1 can be expressed as in Ref. 6. The classical dynamics for the in-plane spin fluctuations follows from[6]

$$\dot{\varphi}_\alpha = \frac{1}{S\mu_\alpha}\frac{\partial H}{\partial m_\alpha} = \sum_{\alpha'} \mathcal{F}_{\alpha,\alpha'} m_{\alpha'} \qquad (7)$$

and a similar equation for $\dot{m}_\alpha$. The mode frequency goes to zero when the determinant of $\mathcal{F}$ goes to zero, which gives the condition for finding a critical anisotropy. This was performed by setting up the matrix $\mathcal{F}$ numerically for a number of rings N, and using a secant search method, adjusting λ or d while holding the other fixed, until a zero determinant resulted.

4. Critical Anisotropies–Numerical Results

For a total number of rings $N \leq 3$, one can easily write down explicitly the total ring energy and matrix $\mathcal{F}$, and determine critical anisotropies analytically, as was done by Zaspel et al[8] for the square lattice vacancy problem. The vacancy-influenced critical exchange anisotropy $\delta_{cv} = 1 - \lambda_{cv}$ is found for null single-ion anisotropy, $d = 0$. The vacancy-influenced critical single-ion anisotropy d_{cv} is found for null exchange anisotropy, $\delta = 0$ or equivalently, $\lambda = 1$. The results from a C-program for the N-ring calculation agreed with the analytic calculations for $N \leq 3$ on all three lattices, verifying the reliability of the program. Obviously, the critical values depend on N, therefore, results were obtained for a range of N up to the order of 1000 rings until convergence of λ_{cv} and d_{cv} to 10 significant figures. A smaller number of rings ($N \approx 400$) is necessary to achieve this for the triangular lattice, probably because it is denser. A summary of the results is shown in Tables I, II, and III. On the square and hexagonal lattices, the calculation gives no solution for either critical anisotropy at $N = 1$. On all the three lattices, a minimum number of rings is necessary before the critical anisotropies even move into the easy-plane range ($\lambda_{cv} < 1$ and $d_{cv} > 0$).

The converged critical exchange anisotropies are $\delta_{cv} \approx 0.0261392320, 0.0455022615, 0.0606587833$, for hexagonal, square and triangular lattices, and the corresponding single-ion critical anisotropies are $d_{cv} \approx 0.03674492096, 0.0824221891, 0.1608450953$. Just as found for a vortex centered in a plaquette, the critical anisotropies increase with the coordination number, and the single-ion critical value is larger than the exchange value. The results confirm and expand upon those found by Zaspel et al.[8] Most importantly, a vortex on a vacancy will tend to be stabilized in the planar form, even at fairly weak anisotropy that would otherwise produce stable out-of-plane vortices far from any vacancies. The numerical values for the square lattice are slightly different here due to using the energetically relaxed in-plane vortex profile (not Eq. 3), and, calculations to a large number of rings until convergence, rather than an extrapolation procedure from a small number of rings.

TABLE I: **Hexagonal lattice** critical anisotropy parameters for a relaxed vortex on a vacancy as a function of the number of rings N and system radius R.

N	R/a	λ_{cv}	d_{cv}
2	1.732	1.5636211762	-0.38565740698
3	2.000	1.2077648210	-0.20076947906
4	2.646	1.1101053643	-0.11918190977
10	4.359	1.0023063573	-0.00297428015
11	4.583	0.9962392581	0.00492191196
20	6.245	0.9800726402	0.02721911999
100	15.000	0.9738836510	0.03669965239
400	30.643	0.9738607689	0.03674491810
1500	60.108	0.9738607680	0.03674492096
3000	85.497	0.9738607680	0.03674492096

TABLE II: **Square lattice** critical anisotropy parameters for a relaxed vortex on a vacancy as a function of the number of rings N and system radius R.

N	R/a	λ_{cv}	d_{cv}
2	1.414	1.4137593264	-0.4065927450
3	2.000	1.2807409281	-0.3077361144
4	2.236	1.0608891919	-0.0871050739
6	3.000	1.0227216056	-0.0346427396
7	3.162	0.9944246293	0.0089633765
10	4.123	0.9722646499	0.0469741982
100	15.00	0.9544993839	0.0824157890
400	30.89	0.9544977384	0.0824221893
800	44.05	0.9544977385	0.0824221891
1500	60.80	0.9544977385	0.0824221891

B. Relaxed Vortices' Energy and Magnetization

It is interesting to confirm the locations of the critical anisotropies by analyzing the total energy and total out-of-plane magnetic moment of a relaxed vortex, both as functions of anisotropy. A vortex is considered as above, at the center of a circular system centered on a vacancy. The in-plane and out-of-plane spin components

TABLE III: **Triangular lattice** critical anisotropy parameters for a relaxed vortex on a vacancy as a function of the number of rings N and system radius R.

N	R/a	λ_{cv}	d_{cv}
1	1.000	1.8660254038	-0.8660254038
2	1.732	1.2709004131	-0.4284919249
3	2.000	1.0669263945	-0.1342143055
4	2.646	0.9969826115	0.0068108464
10	4.583	0.9454955504	0.1397956043
200	24.43	0.9393412168	0.1608450949
400	35.04	0.9393412167	0.1608450953
800	50.21	0.9393412167	0.1608450953

both were allowed to vary, until a local minimum energy configuration for H was obtained. In actual practice, the minimizing configuration was found by using the original lattice spin fields $\vec{S}_{\mathbf{n}}$ and iteratively repointing each along the effective local field $\vec{F}_{\mathbf{n}}$ due to its neighbors,

$$\vec{F}_{\mathbf{n}} \equiv -\frac{\partial H}{\partial \vec{S}_{\mathbf{n}}} = J\left[\sum_{\mathbf{a}}\left(\vec{S}_{\mathbf{n}+\mathbf{a}} + \delta\ S^z_{\mathbf{n}+\mathbf{a}}\hat{z}\right) + 2d\ S^z_{\mathbf{n}}\hat{z}\right] \tag{8}$$

Scanning linearly through the lattice, each site was updated in sequence, being reset along the net field due partly to some unchanged neighbors and some that have already been repointed. This gives slightly faster convergence than a synchronized global update.

Due to the planar symmetry of H, if all spins are initially set in the xy plane, they will remain precisely in the xy plane under this algorithm, even in a situation where, for example, a planar vortex would be unstable. Therefore, in order to allow for the possibility to relax either to a planar or out-of-plane vortex form, nonzero initial values $S^z_{\mathbf{n}} = 10^{-3}$ were set, together with initial in-plane vortex angles given by Eq. (3). In situations where an in-plane vortex is stable, the S^z spin components decay away to zero; conversely, at anisotropy where an out-of-plane vortex is stable, the S^z components grow into the appropriate out-of-plane vortex profile. The iterations were allowed to proceed until the average spin changes per site fell below a desired level, typically on the order of 1 part in 10^{16}. By the time the individual spin changes reached this size, the energy converged to an even higher precision. It is interesting also to note that this iteration converges all the more slowly as the anisotropy comes closer to a critical value, a characteristic feature related to the slow dynamics of the soft mode responsible for the in-plane to out-of-plane instability.

In a finite system, the boundary can either enhance or diminish the ability of nearby spins to tilt out of the easy plane, affecting the calculated critical anisotropy values, as seen above. For all three lattices studied, fairly good convergence of critical values took place below a system radius $R = 50a$. Therefore we calculated relaxed vortex states for systems with $R = 50a$; the spins at the edge of the system have no constraint from outside, that is, a free boundary condition holds. The energy was calculated relative to the ground state energy for spins aligned within the xy plane, an amount of $-JS^2$ per exchange bond. In addition to the energy, the total magnetic moment was calculated, having only a z component: $M = \sum_{\mathbf{n}} S^z_{\mathbf{n}}$. Its deviation from zero gives a distinct signature for the transition to an out-of-plane state.

Results are presented here using exchange anisotropy only, setting the single-ion anisotropy to zero. The vortex magnetic moments M found as a function of λ are shown in Fig. 4. The critical anisotropies obtained by numerical relaxation of the vortex structure, and observed in this graph, confirm to several digits the critical anisotropies determined in Sec. III A 4. The same data is replotted in the inset of Fig. 4 versus scaled anisotropy $\lambda - \lambda_{cv}$, using the precise critical values from Sec. III A 4. One sees that once λ passes λ_{cv}, the magnetic moment grows initially proportional to $\sqrt{\lambda - \lambda_{cv}}$, and fastest on the more open hexagonal lattice, and slowest on the denser triangular lattice. There is a corresponding extremely soft change in the total system energies (relative to the planar vortex energy E_P) as shown in Fig. 5, verifying that the out-of-plane transition is towards a vortex of lower energy, once the anisotropy becomes weaker than the critical strength. Some typical out-of-plane vortex profiles are exhibited in Fig. 6, indicating not only the growth of total M with deviation from critical anisotropy, but also an associated increase in the vortex radial length scale as the anisotropy *strength* diminishes. Figure 6 also lends support for Zaspel et al's explanation for the lowering of the critical anisotropy strengths due to the presence of the vacancy. The missing bonds reduce the total energy of both types of vortices, however, the in-plane vortex energy is reduced more than the typical out-of-plane vortex energy (except at rather weak anisotropy) because the (removed) out-of-plane tilted exchange bonds were relatively smaller energy contributions than if they had been lying purely in-plane. This is true on all the lattices studied, the differences between them being caused by the different densities (sites per unit area).

IV. VORTEX-VACANCY INTERACTION POTENTIAL

The above analysis requires that a vortex is actually attracted energetically to a vacancy. This is a reasonable supposition; the missing bonds clearly reduce the total system energy, and especially the exchange energy due to the in-plane components if the vortex is centered on the vacancy, because the spins near a vortex core are the most strongly misaligned ones. A lesser reduction in in-plane exchange energy results if the vortex is near the vacancy but not exactly centered on it. Therefore one can conclude that there should be an attractive potential pulling a vortex into a vacancy site. (Mól et al[12] came to a different conclusion, estimating a repulsive potential

between a vortex and vacancy in a continuum model.) Due to its intrinsic interest as well as the implications for the acceptable interpretation of the vacancy modified critical anisotropies, an analysis of the interaction potential between a vacancy and a vortex (in a lattice system) is called for. Therefore we investigate further the vortex-vacancy energetics, especially as a function of their separation.

A. Vortex-on-Vacancy Pinning Energy

As a first step, which suggests clearly that the potential should be attractive, a comparison is made of the energies of a single vortex at the center of a circular system of radius R, in two obvious cases: 1) the lattice is uniform (no vacancy) and the vortex is centered in a plaquette; 2) the vortex is centered on a vacancy at the system center. By using the energy minimizing iterative method [Eq. (8)] just described, the vortex configurations for the two cases are easily obtained, and their energies can be compared. At the same radii R, the two defined systems do not necessarily have the same number of lattice sites or bonds (their lattices are shifted relative to one another and the circular boundary), so the comparison may require careful interpretation. We proceeded by producing a set of energies as a function of system size and compare the two results versus R. In Fig. 7 the comparison is made for *in-plane* vortices on systems with $\lambda = 0$ and $d = 0$; the vortex-on-vacancy energy lies below the vortex-in-plaquette energy for all radii. The difference is the vortex-on-vacancy binding energy or pinning energy, ΔE. For example, for in-plane vortices on the **square lattice**, $\Delta E_{\rm sqr} \approx 3.178 JS^2$, more or less independently of the system size, and independent of the anisotropy as long as the vortices are both of the in-plane type. The in-plane vortices on **hexagonal** and **triangular** lattices indicate binding energies of $\Delta E_{\rm hex} \approx 1.937 JS^2$ and $\Delta E_{\rm tri} \approx 5.174 JS^2$, respectively (for $\lambda = d = 0$). The conclusion is obvious, that if observed in an extended system (aside from possibly strong boundary effects), an in-plane vortex *will* lower its energy by ocurring centered on a vacancy, rather than in a plaquette.

In Fig. 8, a typical comparison is made for *out-of-plane vortices*, using $\lambda = 0.99$ (greater then λ_{cv} on all lattices studied) and $d = 0.0$; again the vortex-on-vacancy energy is lower for all system sizes. (The calculation required a larger system than for $\lambda = 0$ in order to produce stable out-of-plane vortex profiles in a finite radius.) For the square lattice, the vortex binding energy is reduced drastically, to about $0.232 JS^2$; this value is expected to be a function of the anisotropy parameters. One could also consider an alternative situation where the vortex is of out-of-plane form when centered in a plaquette, but destabilizes to in-plane form if centered on a vacancy (whenever $\lambda_c < \lambda < \lambda_{cv}$, such as any of the three lattices studied with $\lambda = 0.93$ and $d = 0$). In this latter example, the vortex-on-vacancy energy is again consistently lower than the vortex-in-plaquette energy at the same radius, indicating once again an energetic attraction to a vacancy. In this case the pinning process also will be associated with a significant signature: the complete *elimination* of the out-of-plane magnetization component.

TABLE IV: Some vortex-on-vacancy binding energies (in units of JS^2) and magnetization reductions (in units of S) estimated by comparing to the vortices-in-plaquette structures ($d = 0$), using circular systems of radius $R \leq 300a$.

λ	$\Delta E_{\rm hex}$	$\Delta M_{\rm hex}$	$\Delta E_{\rm sqr}$	$\Delta M_{\rm sqr}$	$\Delta E_{\rm tri}$	$\Delta M_{\rm tri}$
0.0	1.937	0.0	3.178	0.0	5.174	0.0
0.93	1.486	21.31	1.807	28.05	2.45	32.42
0.99	0.224	24.63	0.232	17.27	0.310	14.85

Binding energies for vortex-on-vacancy pinning are given in Table IV, for the three anisotropy parameters $\lambda = 0$, 0.93, and 0.99, corresponding to permanently in-plane, out-of-plane transforming to in-plane, and permanently out-of-plane vortices. The decrease (ΔM) in total out-of-plane magnetic moment as a vortex is pinned on a vacancy is also summarized there. (ΔM is the difference of the vortex-in-plaquette and the vortex-on-vacancy magnetic moments.) Pinning energies and magnetic moment changes were calculated for systems with radius $R = 100a$, for the full range of easy-plane exchange anisotropy, as displayed in Fig. 9. (As explained above, at this radius, the results do not have any dependence on system size.) At weak anisotropy ($\lambda \to 1$) the pinning energy increases almost linearly with anisotropy strength. The pinning energy saturates at its largest value once $\lambda < \lambda_c$ for the lattice under study; the pinning energy is always highest for the more dense lattices. The magnetization change on pinning is even more interesting. It starts at a nonzero value for the isotropic limit ($\lambda = 1$), reaching a sharp maximum exactly at λ_{cv} for the lattice under study (transition between free out-of-plane vortex and pinned in-plane vortex). Finally ΔM becomes zero at λ_c, where the pinning involves only planar vortices.

The region where the pinning leaves the vortices in out-of-plane form ($\lambda > \lambda_{cv}$) is of special interest; the pinning is associated with relatively small energy change in combination with a significant magnetization change. Such a vortex pinning/depinning transition might be initiated due to thermal fluctuations under appropriate conditions, associated with large out-of-plane magnetization fluctuations. One the other hand, close to the planar limit ($\lambda = 0$), the large pinning energy means that vortices formed thermally will tend to pin on any vacancies present. Free vortex density could be greatly reduced if there is high enough vacancy density.

B. Separated Vortex–Vacancy Potentials

To proceed further, it is necessary to study the energy of a vortex separated from a vacancy by some distance

$r_{\rm vv}$. The energy minimization scheme of Sec. III B is to be applied to different vortex-vacancy arrangements. The potential is considered here for square, hexagonal and triangular lattices. Generally, the interaction potential between the two could depend on the direction relative to the lattice, as well as the radial separation.

In order to investigate this, again a circular system of radius R is used, with a vortex placed at its center, which is the origin of coordinates, $(0, 0)$. The vacancy is placed at some position $\vec{X} = (X_x, X_y)$ which is allowed to vary. Alternatively, if the vortex were placed at different positions away from the system center, a boundary energy that changes significantly with the vortex position would result, regardless of the presence or absence of a vacancy. To avoid this complication, it is much simpler to fix the vortex position at the system center, and move the vacancy around, measuring the total system energy. It is not expected that there is a strong energy change due to the vacancy approaching the system boundary. Therefore, one expects the resulting total energy to give a good indication of the intrinsic vortex–vacancy interaction potential.

What this means in practice is that, with the vortex fixed at the origin (center of circle of radius R), all the lattice sites are allowed to shift as the vacancy takes on a range of positions. This implies that lattice sites periodically pass by the vortex as the vacancy is moved to a sequence of positions. To avoid an undefined in-plane spin direction, a lattice site should not be allowed to fall squarely on the vortex position; as a result, some choices of vacancy position are prohibited.

For this numerical algorithm, it is simple to specify the vacancy position, which influences the positions of the rest of the lattice sites. On the other hand, an exact specification of a desired vortex position is not possible, because the presence of an off-center vacancy near a vortex skews the vortex spin field, leading to an ambiguity in the position of the "vortex center." Indeed, without a sufficient constraint, if an initial nearly in-plane vortex is placed near a vacancy, and then the relaxation procedure already described (Sec. III B) is applied, it is possible that the vortex simply shifts onto the vacant site. Therefore, a method is needed to at least partially enforce some desired vortex position.

The following simple but somewhat arbitrary scheme was applied to enforce a desired vortex core position. Based on the arrangement of the lattice sites near the vortex, which is not necessarily symmetrical, a few spins nearest to the vortex are considered as "core" sites. The in-plane angles of these core sites are not changed by the energy relaxation scheme using Eq. (8). Their $\Phi_{\mathbf{n}}$ are held fixed at the original angles given according to the in-plane profile, Eq. (3), however, their out-of-plane spin components *are* allowed to change. The number of core sites is taken to be $n_c = 6, 4$ or 3 for hexagonal, square or triangular lattices, respectively. While it is somewhat artificial and arbitrary to constrain some spins, it was found to be necessary to maintain the desired vortex position, especially at vortex to vacancy distances less than a few lattice constants. This restriction of some spin movement may affect the final energy, therefore one can only consider this as an estimate of the vortex–vacancy potential. However, at a position of high symmetry, such as the vortex on top of the vacancy, the constraint has no effect.

Obviously this is a rich problem with a wide choice of parameters. One expects the potential to be influenced strongly by the choice of anisotropy constants. Here only systems with exchange anisotropy are studied; one expects the results for single-ion anisotropy to be comparable. Furthermore, there could be notably different behaviors depending on where the chosen anisotropy constant λ lies relative to the vortex-on-plaquette critical anisotropy λ_c and the vortex-on-vacancy critical value λ_{cv}. A particularly interesting and complex case is when λ lies between λ_c and λ_{cv}; the vortex will take an out-of-plane form far from the vacancy, and transform into a planar vortex as it is set closer to the vacancy. For λ smaller than both λ_c and λ_{cv}, the vortex always remains planar. Conversely, for λ larger than both λ_c and λ_{cv}, the vortex always remains out-of-plane, although the magnitude of its out-of-plane moment will change as it moves onto the vacancy position, as already indicated in Table IV.

1. *Vortex Remaining in a Planar State*

For sufficiently strong anisotropy ($\lambda < \lambda_c$), the vortex always remains planar at any vortex–vacancy separation. The parameter choice $\lambda = d = 0$ was used to obtain this. A typical result for the energy is shown in the uppermost curve of Fig. 10, for a square lattice system, with radius $R = 50a$. Curves with essentially the same shapes were obtained also on a system with $R = 30a$, except for an overall shift to lower energies due to the usual logarithmic dependence on system size. One expects that except for fine details (such as the width or depth of the vacancy–vortex potential), the gross features of the potential interaction should not depend on the choice of the lattice (the usual assumption of continuum theory).

The curves in Fig. 10 correspond to vacancy positions along paths in the (10) direction of the lattice, avoiding those points which would cause the vortex to fall exactly on a lattice site. A fairly deep attractive minimum ($\Delta E \approx 3.3JS^2$) is found for the vacancy centered on the vortex, with obvious periodic wings due to the lattice. Similar results are obtained for vortex–vacancy displacements along other directions, but with a slightly different width of the potential minimum (the vortex–vacancy potential is not isotropic). Clearly this confirms the energy deviation found in Sec. IV A, and furthermore, gives an indication of the radial separation over which the vacancy has a strong influence on a vortex (1–2 lattice constants). The periodic variations for large vortex–vacancy separation demonstrate the relatively weaker local potential effects that tend to center a vortex within an individual

plaquette. If one did not constrain the small set of core spins to enforce a desired vortex position off-center in a plaquette, then the relaxation would simply produce a vortex profile centered in the nearest convenient plaquette, and these periodic variations would be greatly reduced. Similar results hold for the hexagonal and triangular lattices, but with potential depths as found in Sec. IV A, and periodic variations in the wings that are distinctive to the lattice. When $\lambda < \lambda_c$, the total out-of-plane magnetization remains at zero for the whole range of vortex–vacancy separations.

2. *Vortex Remaining in an Out-of-Plane State*

It was found above that for out-of-plane vortices, the pinning energy was much weaker than for in-plane vortices. Thus it makes sense also to compare the radial dependence of the vortex-vacancy potential interaction for out-of-plane vortices to that for in-plane vortices.

As an example of this possibility, consider exchange anisotropy constant $\lambda = 0.96$ for the square lattice, larger than the value $\lambda_{cv} \approx 0.9545$, which results in stable out-of-plane vortices regardless of their position. The potential curve for separations along the (10) direction of the lattice is shown in the lowermost curve of Fig. 10. Only slightly different potential curves result for separations along other directions. The potential curve is very smooth compared to that for the in-plane vortices ($\lambda = 0$), which must be due to the relatively low energy out-of-plane tilting adjustments of the spins. The corresponding change in the overall system out-of-plane magnetization is shown in Fig. 11. As the vortex is moved closer to the vacancy, its out-of-plane magnetization diminishes by $\Delta M \approx 30S$ at the same time that its energy is mildly reduced by $\Delta E \approx 1.0JS^2$, with an overall attraction. Of course, the depth of the attraction will depend on the particular choice of anisotropy strength.

If this type of situation holds in a magnetic material, (large change in M associated with small energy difference) there could be large out-of-plane magnetization fluctuations expected as vortices are alternately pinned and freed by vacancies, due to thermal fluctuations. The degree of this effect will be greatest for an anisotropy parameter λ approaching the isotropic limit, $\lambda \approx 1$, corresponding to the largest magnetization *change* together with the smallest energy difference between the free and pinned vortex states. The two different states, however, could be difficult to distinguish in a real medium, because both have nonzero (and large) M.

3. *Vortex Transforming From Out-of-Plane to In-Plane*

Alternatively, consider exchange anisotropy $\lambda = 0.90$ for the square lattice, which is above $\lambda_c \approx 0.7034$ and below $\lambda_{cv} \approx 0.9545$. The vortex–vacancy potential is shown as the middle curve of Fig. 10. At this anisotropy strength, the magnetic moment for the separated out-of-plane vortex is about $M \approx 19S$. As the vortex is pulled closer to the vacancy, it minimizes its energy by reducing the out-of-plane magnetization to zero, transforming dramatically from out-of-plane form to in-plane form (Fig. 11). In the process, one sees an intermediate overall energy reduction of about $2.3JS^2$. If such a transition between the pinned planar and free out-of-plane states could be controlled externally by some applied field, such a pair of states could have practical applications for data storage, especially because of the transition to an easily distinguished zero magnetization state.

V. CONCLUSIONS

A vacancy has been found to have substantial influence on the structure and stability properties of a vortex in an easy-plane magnet. The quasi-static analysis presented here is valid for FM and AFM models on square and hexagonal lattices, and only for the FM model on a triangular lattice. Consistent with the stability results found by Zaspel et al,[8] when a vortex is energetically relaxed centered on a vacancy, relatively weaker easy-plane anisotropy will stabilize it in the planar form, compared to that necessary when the vortex is centered in a plaquette far from any vacancy. This result holds as well on hexagonal and triangular lattices; the critical anisotropy strengths δ_{cv} and d_{cv} are always reduced for vortex-on-vacancy compared to those for vortex-in-plaquette, δ_c and d_c. All the critical anisotropy strengths are smallest on the hexagonal lattice and largest on the triangular lattice, which suggests that the coordination number and lattice density control the effect.

Using a simple scheme to enforce a desired vortex position, energetically relaxed vortex–vacancy configurations were produced. The potential interaction between the two has been estimated for the different lattices and anisotropy regimes. In all cases studied, the vortex–vacancy interaction is attractive. This is important because it establishes the vortex-on-vacancy states as legitimate local minimum energy configurations. The depth of the potential holding a vortex on a vacancy (pinning energy) has been estimated. It tends to be strongest on the triangular lattice and weakest on the hexagonal lattice for in-plane vortices. For out-of-plane vortices, the typical depth of the vortex pinning potential tends to be much weaker than for in-plane vortices. These results are consistent with the attractive pinning potential found for localized solitons in isotropic 2D antiferromagnets studied with a nonlinear sigma model.[15,16]

An interesting effect is expected for a system with anisotropy strength intermediate between the vortex-in-plaquette and vortex-on-vacancy critical anisotropies (for example, $\lambda_c < \lambda < \lambda_{cv}$). In the transformation from out-of-plane to in-plane type as a vortex moves from free to pinned on a vacancy, the out-of-plane magnetization is completely eliminated. This could lead to strong magne-

tization fluctuations, and also be considered as an additional signature of vortices and a distinct signature of the pinning process. Additionally, the magnetic fluctuations associated with pinning and de-pinning of *out-of-plane* vortices may be even stronger: relatively large out-of-plane magnetization changes will occur at very low energy difference between the pinned and free vortex states. The largest magnetization changes in the pinning process occur at the vortex-on-vacancy critical anisotropy, $\lambda = \lambda_{cv}$.

Alternatively, one could consider application of a weak out-of-plane magnetic field, which would bias the out-of-plane polarizations of generated vortices along that preferred direction (generating the "light" cone-state vortices[17,18]). An initial low-temperature state of planar vortices pinned on vacancies could produce de-pinned out-of-plane vortices preferentially with the same polarization, leading to a large macroscopic magnetic moment. This could be a intriguing effect if the de-pinning and pinning of vortices on vacancies could be controlled at will, leading to interesting device possibilities.

Finally, one can speculate on how an attractive potential between vacancies and vortices should affect the statics and dynamics of the BKT topological transition. The MC results by Leonel et al[13] indicated that a small percentage of spin vacancies lowers the transition temperature, which they interpreted to result from a *repulsive* vacancy–vortex potential (under an assumption of a certain vortex deformation caused by a vacancy). The explanation requires that the repulsion produces a greater free-vortex density at a lower temperature, thereby leading to more disorder and a lower transition temperature. Actually, we found here that the vacancies are likely to *attract and pin* any vortices/antivortices that are forming, with fairly strong pinning energies for the planar model, and associated lower vortex formation energies. An improved continuum model for vacancy–vortex interaction, without the assumption of a global vacancy-induced vortex deformation, has verified this attractive potential.[19] At temperatures well below the energy scale of JS^2, nearly all formed vortices should be pinned. Even so, the pinned vortices will lead to long range disorder and the BKT transition, but at a lower temperature, especially because their formation energy is *much lower* than for unpinned vortices. Further detailed MC studies could be interesting if they could demonstrate the respective roles of the free versus pinned vortices, by analyzing their number densities. This question may also be answered by studying the dynamic correlations: the dynamic signatures of free vortices should be distinct from those due to pinned vortices.

---

* Electronic address: wysin@phys.ksu.edu; URL: http://www.phys.ksu.edu/~wysin/

[1] S. Hikami and T. Tsuneto, Prog. Theor. Phys. **63**, 387 (1980); S. Takeno and S. Homma, Prog. Theor. Phys. **64**, 1193 (1980); **65**, 172 (1980).

[2] G.M. Wysin, M.E. Gouvêa, A.R. Bishop and F.G. Mertens, in *Computer Simulations Studies in Condensed Matter Physics*, edited by D.P. Landau, K.K. Mon and H.-B. Schüttler (Springer-Verlag, Berlin, 1988).

[3] M.E. Gouvêa, G.M. Wysin, A.R. Bishop and F.G. Mertens, Phys. Rev. B **39**, 11840 (1989).

[4] G.M. Wysin, Phys. Rev. B **49**, 8780 (1994).

[5] G.M. Wysin, M.E. Gouvêa and A.S.T. Pires, Phys. Rev. B **57**, 8274 (1998).

[6] G.M. Wysin, Phys. Lett. A **240**, 95 (1998).

[7] C.E. Zaspel and D. Godinez, J. Magn. Magn. Mater. **162**, 91 (1996).

[8] C.E. Zaspel, C.M. McKennan and Sabrina R. Snaric, Phys. Rev. B **53**, 11317 (1996).

[9] C.E. Zaspel, J.E. Drumheller and K. Subbaraman, Phys. Stat. Sol. (a) **189**, 1029 (2002).

[10] K. Subbaraman, C.E. Zaspel and John E. Drumheller, Phys. Rev. Lett. **80**, 2201 (1998).

[11] A.R. Pereira and A.S.T. Pires, J. Mag. Magn. Mater. **257**, 290 (2003).

[12] L.A.S. Mól, A.R. Pereira and A.S.T. Pires, Phys. Rev. B **66**, 052415 (2002).

[13] S.A. Leonel, P.Z. Coura, A.R. Pereira, L.A.S. Mól, and B. V. Costa, Phys. Rev. B **67**, 104426 (2003).

[14] V. Berezinskii, Sov. Phys. JETP **32**, 493 (1970); J.M. Kosterlitz and D.J. Thouless, J. Phys. C **6**, 1181 (1973).

[15] L.A.S. Mól, A.R. Pereira and W.A. Moura-Melo, Phys. Rev. B **67**, 132403 (2003).

[16] A.R. Pereira, Phys. Lett. A **314**, 102 (2003).

[17] B. A. Ivanov and D.D. Sheka, Low Temp. Phys. **21**, 881 (1995).

[18] B.A. Ivanov and G.M. Wysin, Phys. Rev. B **65**, 134 434, (2002).

[19] A.R. Pereira, private communication.

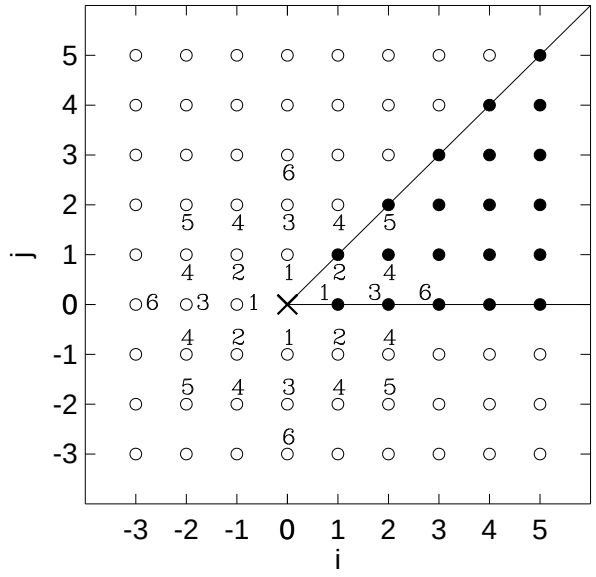

FIG. 1: Vacancy (×) on a square lattice, and surrounding sites which define the (i, j) coordinates of the rings (solid points in first octant are the principal sites). Numbers indicate the symmetry related sites of some of the first few rings. Rings with principal site on one of the symmetry lines at 0° or 45° have four sites; all others have eight.

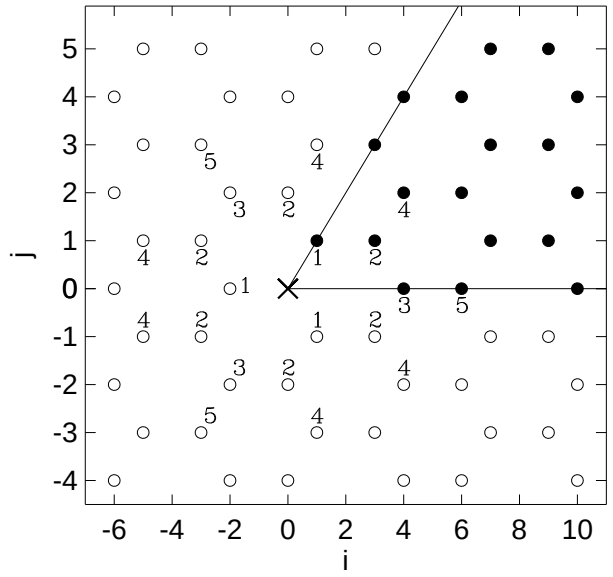

FIG. 2: Vacancy (×) on a hexagonal lattice and definitions of the (i, j) coordinates of some of the first few rings. Rings with principal site on one of the symmetry lines at 0° or 60° have three sites; all others have six.

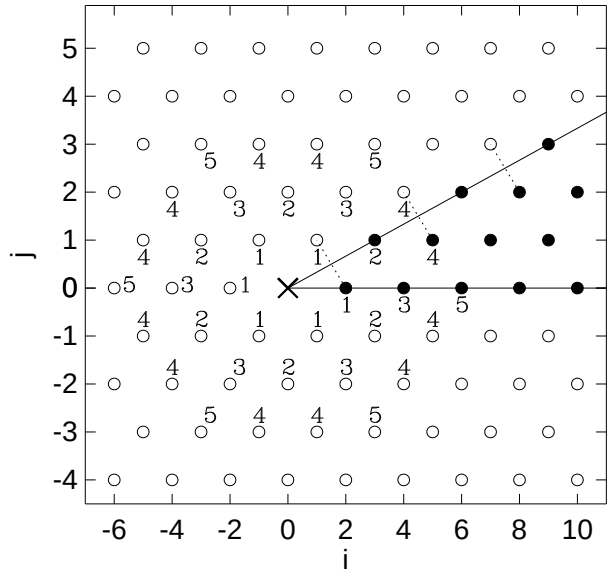

FIG. 3: Vacancy ($\times$) on a triangular lattice and definitions of the (i, j) coordinates of some of the first few rings. Rings with principal site on one of the symmetry lines at 0° or 30° have six sites; all others have twelve. The dashed lines exhibit some of the intra-ring or self-exchange bonds.

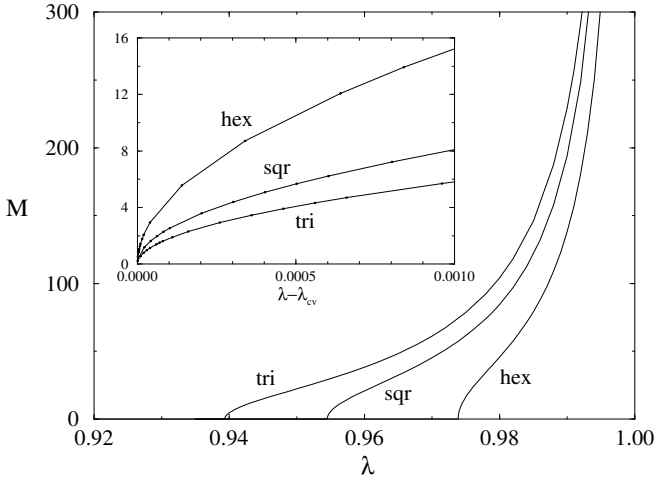

FIG. 4: Total out-of-plane magnetization of a numerically relaxed vortex-on-vacancy versus exchange anisotropy constant λ, for hexagonal, square and triangular lattice systems of radius $R = 50a$ with free boundaries. The inset shows the same data versus shifted exchange anisotropy constants $\lambda - \lambda_{cv}$ near the critical points.

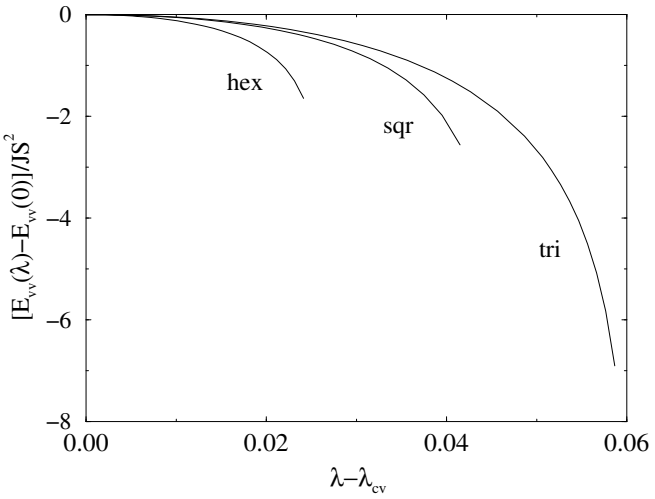

FIG. 5: Energy of a numerically relaxed vortex-on-vacancy relative to in-plane vortex-on-vacancy energies $E_{\rm vv}(0)$ versus shifted exchange anisotropy constant $\lambda - \lambda_{cv}$, for hexagonal ($E_{\rm vv}(0) = 7.143JS^2$), square ($E_{\rm vv}(0) = 13.15JS^2$) and triangular ($E_{\rm vv}(0) = 23.46JS^2$) lattice systems of radius $R = 50a$ with free boundaries.

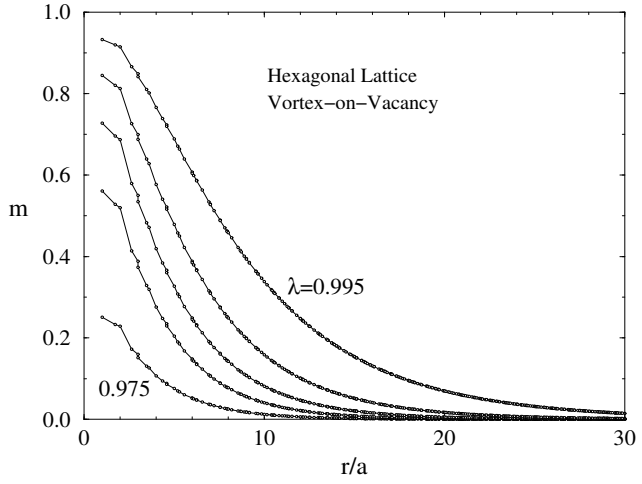

FIG. 6: Radial dependences of the out-of-plane component of numerically relaxed vortex-on-vacancy structures, at $\lambda = 0.975, 0.980, 0.985, 0.990, 0.995$, on a hexagonal lattice system of radius $R = 50a$ with free boundaries.

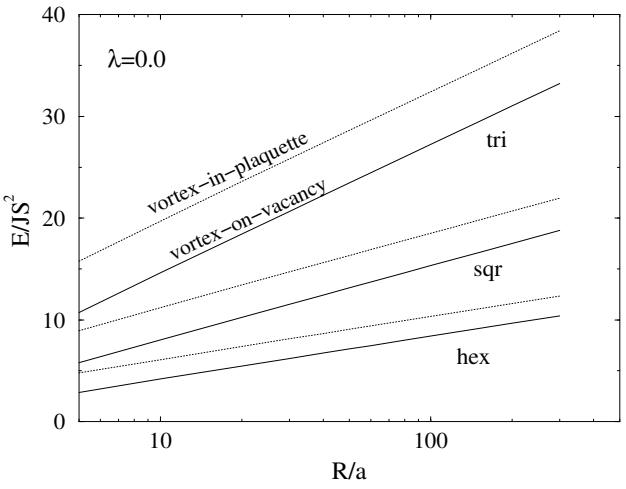

FIG. 7: Comparison of vortex-in-plaquette energies (dotted) with vortex-on-vacancy energies (solid) for in-plane vortices ($\lambda = d = 0$) on circular systems of radius R, showing a substantial pinning energy.

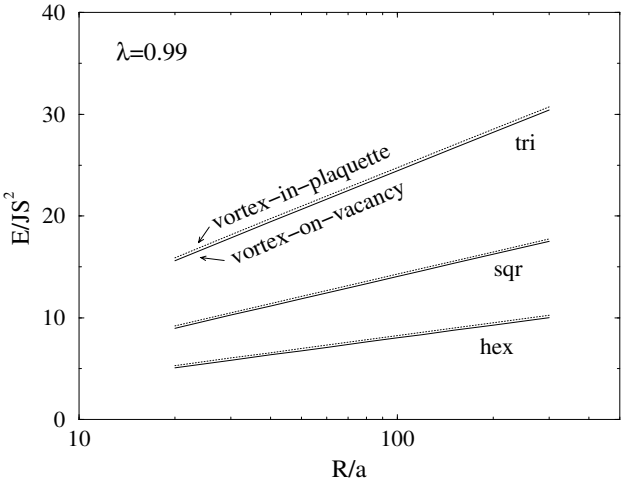

FIG. 8: Comparison of vortex-in-plaquette energies (dotted) with vortex-on-vacancy energies (solid) for out-of-plane vortices ($\lambda = 0.99$, $d = 0$) on circular systems of radius R, showing a very weak pinning energy (See Table IV.).

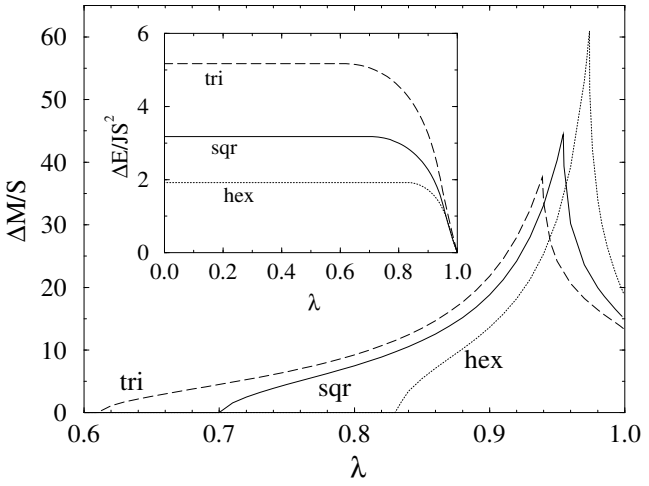

FIG. 9: The changes in vortex out-of-plane magnetic moment (ΔM) and in vortex energy (ΔE, in inset) when a vortex is pinned on a vacancy (changing from centered in a plaquette to centered on a vacancy), as functions of easy-plane anisotropy parameter on hexagonal, square and triangular lattices.

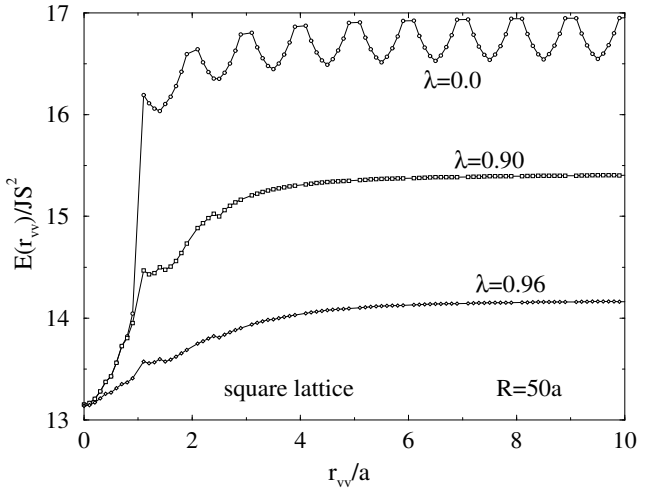

FIG. 10: Vortex–vacancy total energy as a function of their separation $r_{\rm vv}$, calculated on a square lattice system of radius $R = 50a$ for indicated exchange anisotropies ($\lambda = 0$, in-plane; $\lambda = 0.90$, transition from in-plane to out-of-plane with increasing $r_{\rm vv}$; $\lambda = 0.96$, out-of-plane vortices). With the vortex at the origin $(0, 0)$, the vacancy was placed at a sequence of positions in the (10) direction.

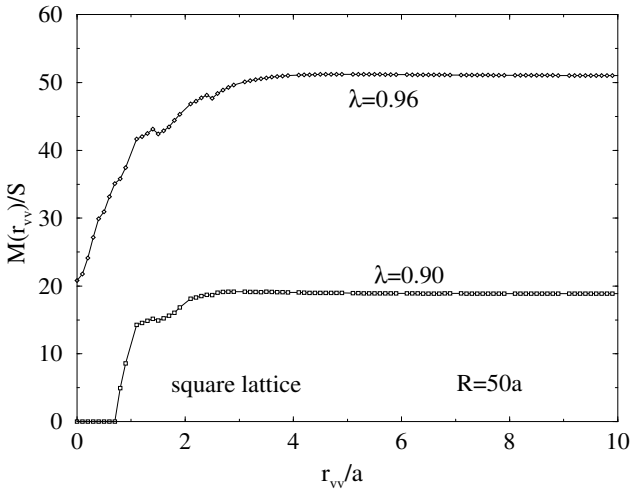

FIG. 11: Vortex–vacancy total out-of-plane magnetization as a function of separation $r_{\rm vv}$, for square lattice systems of radius $R = 50a$ as in Fig. 10. ($M = 0$ for all $r_{\rm vv}$ at $\lambda = 0$.)